Impact of Various Mach Number and AOA on Concave Blunt Nose with Spike Angle Fifteen Degree

[1]Channaveerayya, [2]Mahesh, [3]Srikanth

[1,2]Department of Mechanical Engineering, Government polytechnic Kalagi, Karnataka, India.
[3]Department of Mechanical Engineering, Government polytechnic Bidar, Karnataka, India.

Abstract-
To analyze fluid dynamics around a blunt nose with various spikes and angles of attack, you must first understand how the nose's shape and orientation affect airflow and aerodynamic forces such as lift and drag. Begin by figuring out the shape of the blunt nose and the spikes that will be attached to it. This entails describing the spikes' diameters, shapes, and positions in relation to the blunt nose. Use a CFD software program such as ANSYS Fluent, COMSOL Multiphysics, or OpenFOAM to simulate flow around the blunt nose with different spike configurations. Compare the performance of different spike designs and angles of attack using metrics such as lift, drag, and aerodynamic efficiency. Determine which combinations produce the required aerodynamic properties for the given application. Based on the simulation results, adjust the blunt nose and spikes to improve aerodynamics, reduce drag, or achieve other design objectives. According to the information provided, blunting an aircraft's front surface provides thermal protection. Despite this blunting, the nose still experiences intense thermal activity, necessitating significantly more thermal protection than the rest of the vehicle. To address the issue of wave drag, which is frequently caused by the blunt nose form, changes to the flow field in front of the vehicle are required. One way to make this change is to use a retractable nose spike. By deploying a retractable spike, the flow field can be altered, potentially reducing wave drag and improving aerodynamic performance.

Keywords: Concave Blunt Nose, Spike angle, CFD, Lift force, Mach number, drag force.

1. INTRODUCTION

Fluid dynamics is a sub-discipline of the field of fluid mechanics that studies fluid flow: liquids and gases in motion. It encompasses several sub-disciplines, such as aerodynamics (the study of gases in motion) and hydrodynamics. Fluid dynamics is used in a variety of applications, including calculating aircraft forces and moments, determining the mass flow rate of petroleum through pipelines, forecasting weather patterns, and reportedly modeling fission weapon detonation. Some of its principles are even applied to traffic engineering, where traffic is viewed as a continuous fluid. Fluid dynamics provides a systematic structure that underpins these practical disciplines and incorporates empirical and semi-empirical laws derived from flow measurement that are applied to solve practical problems. A fluid dynamics problem is typically solved by calculating the fluid's various properties, such as velocity, pressure, density, and temperature, as functions of space and time.

A drag-minimizing A device called an aero-spike is intended to reduce blunt body pressure drag at supersonic speeds. In front of the body, the aerospike produces a disconnected shock. A zone of recirculating flow forms between the shock and the forebody, reducing drag and creating a more streamlined profile. It is thought that this concept, which was first applied to the Trident missile, increased range by 550 kilometers. The Trident aero-spike is an extendable boom with a flat circular plate attached. It is deployed as soon as the missile launches from the submarine and breaks through the water's surface. The aero-spike made it possible to have a blunter nose shape, which increased internal volume for propulsion and cargo while lowering drag. This was required because the Trident IC-4, which replaced the Poseidon C-3 missile, had a third propulsion stage that allowed it to achieve the necessary range increase. The third stage motor had to be positioned in the center of the post-boost vehicle, with the reentry vehicles arranged around it, in order to fit inside the current underwater launch tubes. Drag is an important factor to take into account when a body is moving. The drag an automobile experiences increases with speed. It is the resistance to vehicle motion brought on by numerous factors. Drag's source can be used to categorize it. Wave drag, friction drag, pressure drag, induced drag, form drag, and profile drag are a few of these. Since wave drag is pertinent to the current case study, only it has been studied here. The drag force that develops during the formation of a shockwave is known as wave drag.

Wave drag on a body in hypersonic flow is a vital and fundamental aerodynamic problem. To reduce the heating problem, which is most noticeable during the ascent portion of the flight, a blunt body with a large nose radius is required. This causes more wave drag on the vehicle. This wave drag, which is critical in hypersonic flow, must be reduced in order to maximize the thrust of the propulsive system while keeping fuel consumption and propulsive system needs low, hence enhancing the vehicle's payloads and structural integrity. Fuel accounts for over half of the aircraft's basic weight, and a 1% reduction in drag increases the vehicle's payload capacity or range by around 10%.

2. LITERATURE REVIEW

In CFD simulation, structured and unstructured mesh generation techniques are crucial meshing methods. These techniques are occasionally combined to create hybrid grids, also known as chimera, composite, or patched grids. The benefits and drawbacks of each of these approaches have been covered in this article [1]. At nodes within each cell, the solution to a flow problem (velocity, pressure, temperature, etc.) in a finite volume formulation is obtained. The number of cells in the grid affects a CFD solution's accuracy [2, 20]. For a body moving, drag is a crucial factor to take into account. The drag acting on the vehicle increases with vehicle speed. It is the resistance resulting from various sources when the vehicle moves. Drag can be categorized according to where it comes from [3]. A shock wave forms in front of a blunt body when it is passed by a supersonic flow. Since this type of shock wave forms at an angle to the blunt body's surface, it is known as an oblique shock wave. The field of Computational Fluid Dynamics (CFD) [5, 6, 7] began to gain prominence with the steady development of high-speed computers and effective numerical algorithms. Fluid dynamics theory and experimentation are enhanced by CFD, which offers an affordable alternative for simulating actual flows. It has been confirmed that the analytically available solution can be used in practical as it gives the acceptable results [9]. Therefore with the grid independence studies, the numerical results can be compared with the available analytical results, in turn one can validate a CFD tool for solving shock capturing problems. A rapid geometry engine (RAGE) has been developed to allow for preliminary design analysis without labor-intensive CAD support. The geometry tool builds complex aircraft configurations using a component-based approach. Basic algorithms for creating the primary components are presented and discussed [18]. A select geometry model is analyzed with several aerodynamic analysis methods ranging in fidelity to further demonstrate the versatility of the geometry tool.

3. COMPUTATIONAL MODEL

To simulate a test case on a digital computer, it is essential to have enough geometric information about it. The fluid domain is a nearly cut region of the whole system whose outer boundaries are chosen so as not to interfere with the physics of the problem. The fluid surrounding the geometry (external flow issues) is the computational domain in all of the current case studies. It is customary to increase the shock capturing up to 8–10 times the body width or base diameter in the upstream zone and 3-5 times in the distant field.

I

t should be noted that since all of the current case studies involve exterior flow concerns, only the fluid domain—and not the solid body—is being modeled. The present case studies employ symmetrical models. The blunt cone body is modeled for flow at zero angle of attack and two non-zero angles of attack (5 degrees and 15 degrees) for both scenarios (without and with spike).

Figure 1 shows how the ICEM CFD industrial standard code was used to create the 2-D shape of a blunt body. Geometric data for blunt bodies with and without spike arrangements are shown in Figure 2.

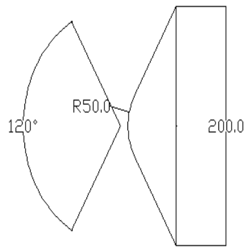

Fig. 1 : Blunt body without spike configuration

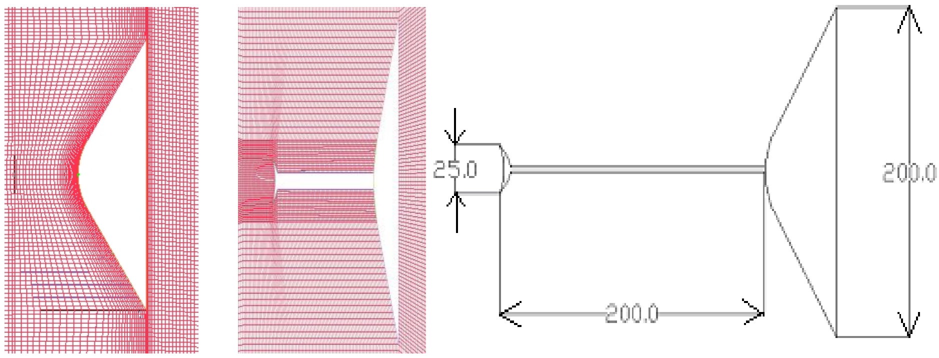

Fig. 2 : Meshed model for Blunt nose, Concave and concave spike configuration

4. PROBLEM STATEMENT

The governing equations have to be satisfied inside the fluid, and specific solutions can only be obtained by defining the initial condition of the flow field and the flow geometry constraint. Therefore, in order to integrate the governing equations, velocity, pressure, and temperature must be appropriately determined at the region's border. When something is transitory, the dependent variable's value at time t=0 needs to be specified, and the time derivative is of first order. We refer to this as the initial condition. Additional restrictions placed on the physical boundaries of the fluid region are referred to as boundary conditions. But in this instance, steady state is taken for granted, so no initial conditions are applied. Velocity, pressure, and temperature are the usual parameters used here to represent the air conditions at an elevation of 5 kilometers (16404 feet) above sea level. It leads to a background outlet. The output of the computational domain is projected to all variables from the interior domain. Wall: The fluid is thought to stick to the wall because of its viscosity on the blunt body's solid surface. This requirement that the solid and adjacent fluid have no velocity in relation to one another is called the no-slip condition. Consequently, the fluid is regarded as non-slippery and the wall boundary condition is applied to the blunt cone model surfaces.

The Continuity Equation: $$\frac{\partial \bar{U}_j}{\partial x_j} = 0$$

The Momentum Equation: $$\frac{\partial}{\partial t}(\rho \bar{U}_i) + \frac{\partial}{\partial x_j}(\rho \bar{U}_i \bar{U}_j) = -\frac{\partial \bar{P}}{\partial x_i} - \frac{\partial}{\partial x_j}\left(\bar{\tau}_{ij} + \rho \overline{u_i'' u_j''}\right)$$

The Energy Equation: $$\frac{\partial}{\partial t}(\rho \bar{h}) + \frac{\partial}{\partial x_j}(\rho \bar{U}_j \bar{h}) = -\frac{\partial}{\partial x_j}\left(Q_j + \rho \overline{u_i'' h'}\right)$$

5. CFD RESULTS AND DISCUSSIONS

The various variable contours for the concave spike attached to the blunt body, with a 15 degree angle of attachment (AOA) and speeds of 2.0 and 4.0 mach, are displayed below in Figures 3 and 4. The distribution of pressure around the blunt body and concave spike is depicted by the pressure contours. A body-fitted shock is reported to have formed directly in front of the concave spike. This suggests that the shock wave is closely tracing the spike's form. Furthermore observed is the successful occurrence of flow separation at the location of the blunt wall. A decrease in the force applied to the blunt wall as a result of this separation may lessen aerodynamic drag. The peak pressure contour is seen to be captured upstream of the spike. This suggests that the highest pressure occurs in this region, likely due to compression effects caused by the spike's shape and the incoming flow conditions. This increased pressure could have implications for aerodynamic performance and structural loading.

5.1 Concave spikes 15 deg AOA and 2.0 Mach

Velocity, Pressure, Density, Temperature Contours & Velocity Vectors, Streamlines plots

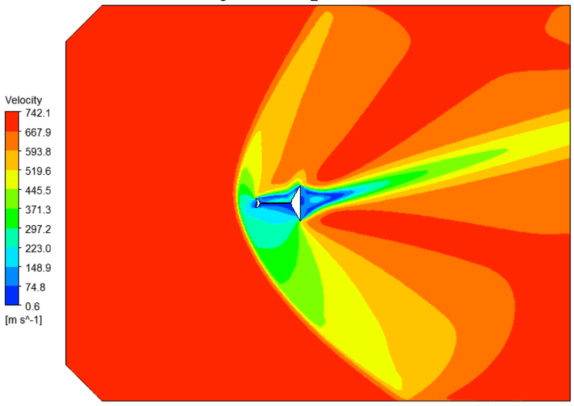

a. Velocity contours

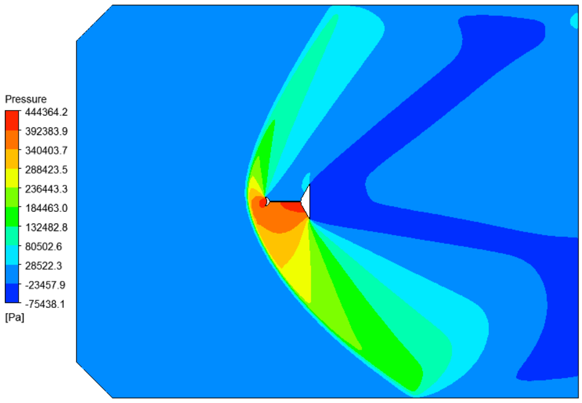

b. Pressure contours

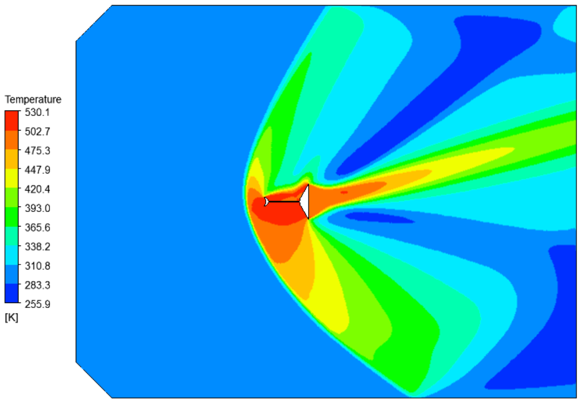

c. Temperature contours

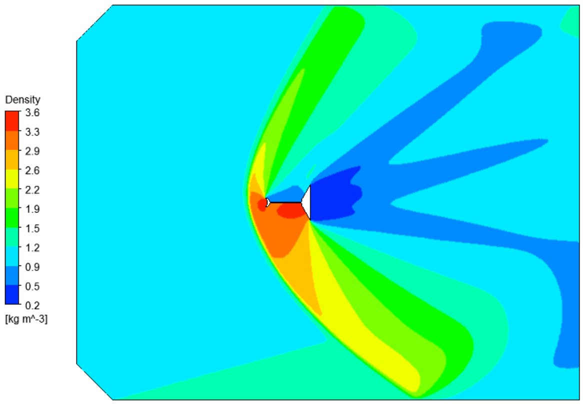

d. Density contours

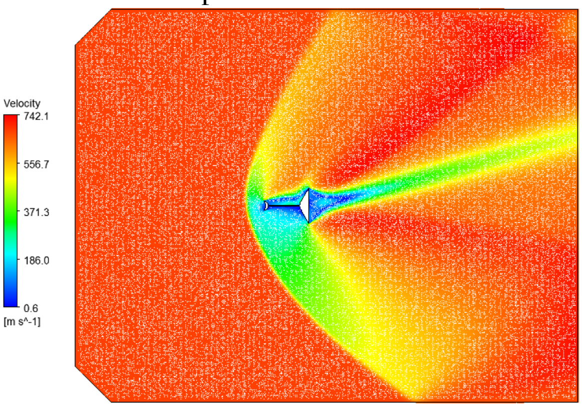

e. Velocity Vectors

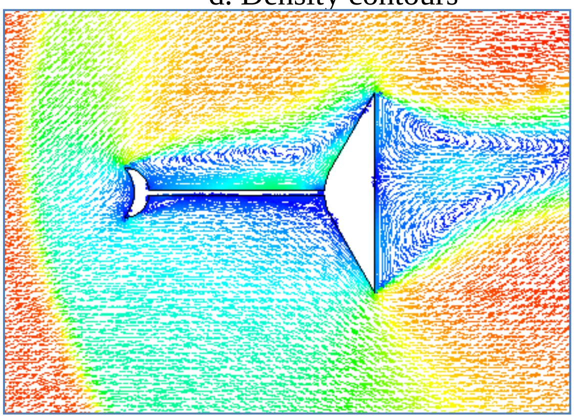

f. Zoomed view

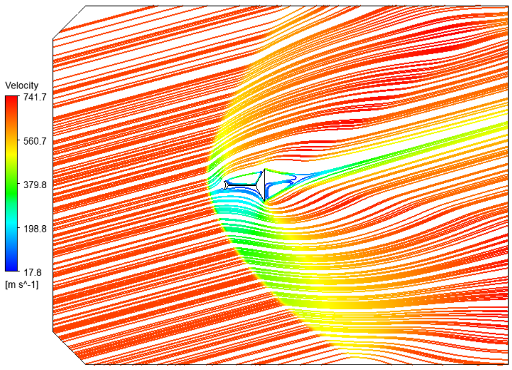

g. Velocity Streamlines

Fig. 3 : Concave spike blunt nose fluid behavior for 2 Mach speed and 15 deg AOA

Above figure shows the different variables contours at 15 deg AOA for 2.0M speed, in the pressure and velocity contours it can be seen that the flow streams are separated due to convex spite at upstream of blunt face. Shock waves are asymmetry. Since flow passes 15 deg inclined direction with high speed, lower part of blunt seeks higher shock waves than upper part. Similarly Temperature, Density contours are captured and there is no disturbance for free stream flow.
Vector plot for convex spikes of blunt nose body is shown in figure. It can be seen that the speed and direction of moving fluid is at 15 deg inclined movement and fluid striking the spike and flow separates successfully. So that peak fluid force appears on lower part of blunt surface. Air recirculation at downstream is tilted. And similar flow patters can be seen in streamline plot.

5.2 Concave spikes 15 deg AOA and 4.0 Mach

Velocity, Pressure, Density, Temperature Contours & Velocity Vectors, Streamlines plots

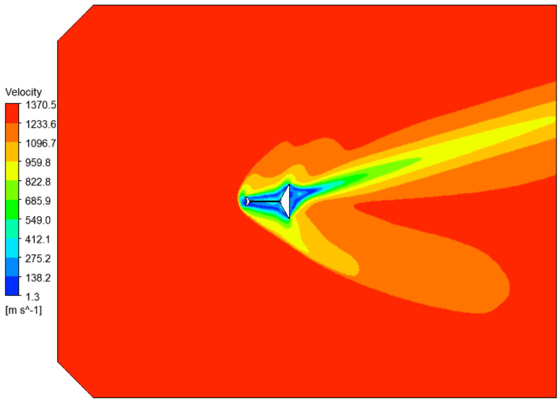

a. Velocity contours

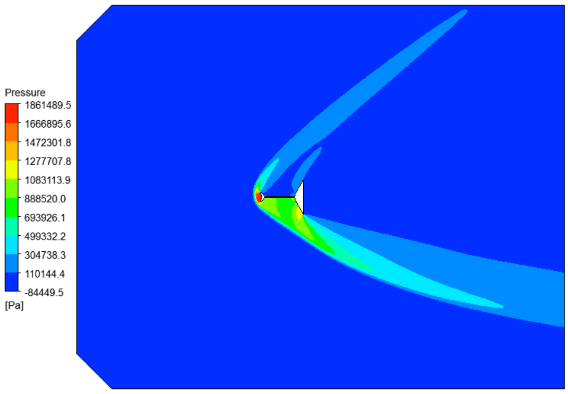

b. Pressure contours

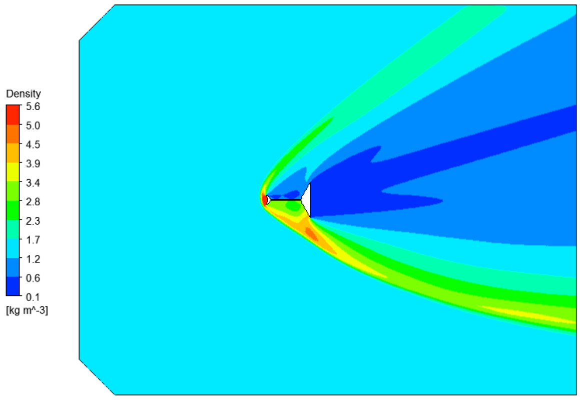

c. Temperature contours

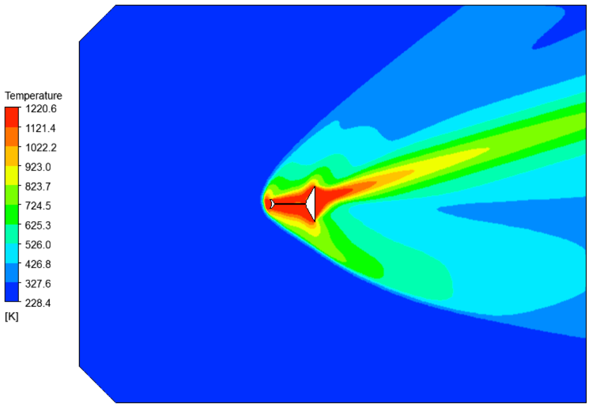

d. Density contours

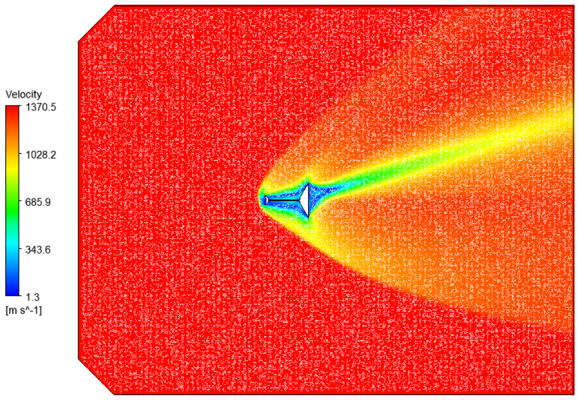

e. Velocity Vectors

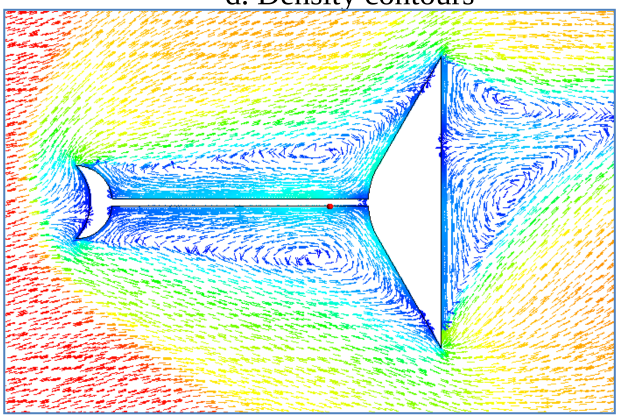

f. Zoomed view

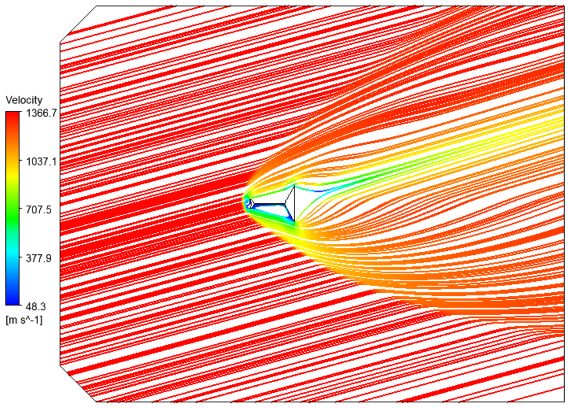

g. Velocity Streamlines

Fig. 4 : Concave spike blunt nose fluid behavior for 4 Mach speed and 15 deg AOA

Above figure shows the different variables contours at 15 deg AOA for 4.0M speed, in the pressure and velocity contours it can be seen that the flow streams are separated due to convex spite at upstream of blunt face. Shock waves are asymmetry. Since flow passes 15 deg inclined direction with high speed, lower part of blunt seeks higher shock waves than upper part. Similarly Temperature, Density contours are captured and there is no disturbance for free stream flow.

Vector plot for convex spikes of blunt nose body is shown in figure. It can be seen that the speed and direction of moving fluid is at 15 deg inclined movement and fluid striking the spike and flow separates successfully. So that peak fluid force appears on lower part of blunt surface. Air recirculation at downstream is tilted. And similar flow patters can be seen in streamline plot.

6. CONCLUSIONS

This spike effectively moves the flow re-attachment point away from the model when it is attached to a blunt cone. It does this by changing the shock structure, which lowers the drag coefficient and lessens wave drag. After comparing different spike configurations, it was discovered that the spike with the flat disc-shaped, concave tip showed the greatest potential for lowering wave drag. Based on the drag coefficient and the percentage of drag reduction seen with various spike configurations, this conclusion was made. The way the spike is shaped affects how the flow field around the blunt body is modified. The concave and flat disc-shaped spike configuration, in particular, was found to be useful in minimizing the negative effects of shock waves on aerodynamic performance by pushing the re-attachment point away from the model. According to the research, choosing the right spike shape can greatly lower drag coefficients and improve the blunt body's aerodynamic efficiency. The disc-shaped spike, which is concave and flat, shows great promise because it can modify the shock structure and lessen wave drag. All things considered, your analysis emphasizes how crucial spike configuration is to enhancing aerodynamic performance, especially when it comes to lowering wave drag on blunt bodies. The design of aerospace vehicles could be optimized with the help of this information, increasing overall efficiency.

REFERENCES:

1. Mark Filipiak, Mesh Generation, Version 1.0, Edinburgh Parellel Computing Centre, University of Edinburgh, November-1996.
2. H. K. Versteeg & W. Malasekera, An introduction to Computational Fluid Dynamics-The finite volume method, Pearson Prantice Hall, 1995.
3. John. D. Anderson, Jr, Fundamentals of Aerodynamics, McGraw Hill International Editions, 1985.
4. H W Liepmann & A Roshko, Elements of Gas Dynamics, John Wiley & Sons, Inc. – Galcit Aeronautical series, 1965.
5. John. D. Anderson, “Computational Fluid Dynamics – the basics with applications”, McGraw Hill Inc, 1985.
6. Joel. H. Ferziger and Milovan Peric, “Computational Methods for Fluid Dynamics”, 3rd revised edition, Springer Verlag publications, 2003.

7.C. A. J. Fletcher, Computational techniques for fluid dynamics – 1, fundamental and general techniques, 2nd edition, 1990.
8.J.F.Thompson, A composite grid generation code for general 3D regions — the Eagle code, AIAA J., Vol. 26 (3) pp.271-272 (1988).
9.S. W. Yuan, "Foundations of fluid mechanics", PHI Publications, 1988.
10.K. Muralidhar & T. Sundararajan, Computational fluid flow and heat transfer, Narosa publishing house, 1984.
11.Pradip Niyogi, S. K. Chakrabartty, M. K. Laha, Introduction to Computational Fluid Dynamics, Pearson Education Series, 2005.
12.S. M. Deshpande & S. V. Raghuramarao, "Numerical methods for compressible flows based on kinetic theory of gases", AR & DB Centre of Excellence for Aerospace CFD, IISc – Bangalore, July 2002.
13.Viren Menezes - PhD thesis, Investigation of aero-spike induced flow field modifications around large angle blunt cone flying at hypersonic mach number, Aerospace Engg Dept, IISc – Bangalore, Feb-2003.
14.K.Sateesh, P.S.Kulkarni, G. Jagadeesh, M. Sun, K. Takayama, Experimental and numerical studies on the use of concentrated energy deposition for aerodynamic drag reduction around re-entry bodies, AIAA, CFD Conference USA.
15.J.S.Shang, Plasma injection for hypersonic blunt body drags reduction, AIAA Journal, Vol.40 No-6, June 2002.
16.K. Satheesh, G. Jagadeesh and P. S. Kulkarni, Hypersonic wave drag reduction in re-entry capsules using concentrated energy deposition, ISSW24, July 12 – 19th, 2004, Beijing, China.
17.Snežana S. Milićev1, Miloš D. Pavlović1, Slavica Ristić2, Aleksandar Vitić2, ON THE INFLUENCE OF SPIKE SHAPE AT SUPERSONIC FLOW PAST BLUNT BODIES, University of Belgrade, Faculty of Mechanical Engineering 27 marta 80, 11000 Belgrade, Yugoslavia
18.David L. Rodriguez* and Peter Sturdza2†, A Rapid Geometry Engine for Preliminary Aircraft Design, Desktop Aeronautics, Inc., Palo Alto, CA, 94301
19.A.N. Volkov a, Yu.M. Tsirkunov a, B. Oesterle b,* Numerical simulation of a supersonic gas–solid flow over a blunt body: The role of inter-particle collisions and Two-way coupling effects, International Journal of Multiphase Flow 31 (2005) 1244–1275
20.Timothy, Baker. Mesh generation: Art or science? MAE Department, Princeton University, Princeton, NJ 08540, USA
21.S. P. Kuo1, "Shock Wave Modification by a Plasma Spike: Experiment and Theory", Department of Electrical & Computer Engineering, Polytechnic University, 6 MetroTech Center, Brooklyn, NY 11201, USA. Received October 14, 2004; accepted November 9, 2004